

# Analysis of Electromagnetic Behavior of Permanent Magnetized Electrical Machines in Fault Modes

M. U. Hassan<sup>1</sup>, R. Nilssen<sup>1</sup>, A. Røkke<sup>2</sup>

1. Department of Electrical Power Engineering, Norwegian University of Science and Technology, 7491, Trondheim, Norway.

2. Rolls Royce Marine AS, Jarlevein 8, 7041 Trondheim, Norway.

## Abstract

In this paper, a transient 3D finite element model using COMSOL Multphysics5.2a is presented to test the flux weakening capabilities of Dual Rotor Permanent Magnet Synchronous Machine (DR-PMSM). The DR-PMSM has two rotors instead of one, with identical surface mounted magnets on both rotors. One of these rotors has the capacity to rotate with respect to the other, to reduce the flux or completely short the flux path by re-alignment of rotors. The stator of DR-PMSM is just like a conventional PMSM with concentrated windings.

A 2D FEM model of a conventional PMSM was also built to check the validity and compare the power efficiency of the DR-PMSM. It is seen that torque is proportional to the active length of the machine, and if a gap is introduced between the rotors then the total length of the machine must be increased. Also, the axial flux component which induces eddy currents in the stator teeth was studied. By modeling anisotropy in the stator iron, certain hot spots could be seen in the middle part of the stator. The forces that were in the shifting mechanism were studied and is concluded that the magnetic cogging can should minimized to reduce the effect of these forces.

**Keywords:** Electric Machines, Rotating Machinery, Stator faults, Fault tolerant control, Field Weakening, Anisotropy, Dual rotor, 3D modeling

## Introduction

For propulsion, electric ships use induction motors, synchronous motors or Permanent Magnet synchronous motors. For electric machines 30-40% of faults are related to electromechanical faults i.e. stator winding faults etc.[1] Usually electric machines and drives have very low maintenance requirement. The ship's environment can however make it more prone to failures.

A survey focusing on electric motors used in offshore applications highlights that most faults are due to bearing or stator winding defects[2]. An insulation failure can be catastrophic because it takes around 30 seconds to expand and could lead to destruction of

stator core [3]. Thus, timely detection and mitigation of faults is required before they lead to catastrophic events such as fire on board.

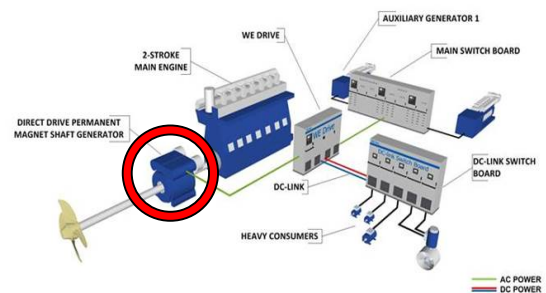


Figure 1 Directly driven on-shaft generator for marine propulsion

Requirements to the generator states that during a stator inter turn fault, the PMSM should be made electrically dead (there should be no flow of power). The propulsion system can be stopped temporarily and after mitigating the fault conditions it should be started again.

## Field Weakening in PMSM

As inter turn faults develop gradually, this gives some time to control and mitigate the faults. To handle this situation a field weakening method using moveable magnets in the rotor was selected.

Field weakening is in a fault situation used to control and limit the induced voltages in the machine. In these PM machines the magnetic field intensity of the PM is normally fixed. To implement field weakening in PM machines, this can be done with currents given by the converters or by changing the Permanent magnet location in the rotor. This paper explores the capabilities of field weakening in such designs using COMSOL for novel DR-PMSM.

## Dual Rotor Permanent Magnet Synchronous Machine (DR-PMSM)

The Dual Rotor Permanent Magnet (DRPM) machine is a novel PM machine with field weakening capabilities. The rotor is divided into two sections, in which each section has identical sets of alternating poles as shown in figure 2a. One of these rotors has the

capacity to rotate with respect to the other rotor part, to reduce the flux by re-alignment of rotor poles. The idea of dual rotor arrangement can be applied to any surface magnet or interior magnet rotor structures.

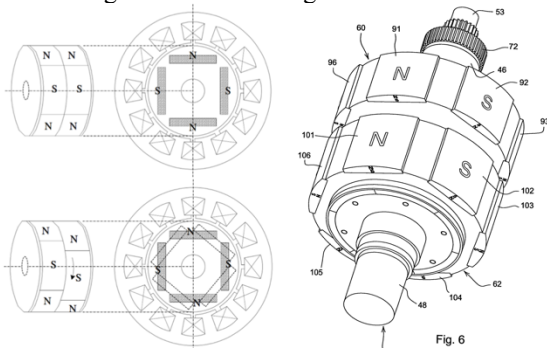


Figure 2 (a) DR-PMSM shifting rotor (b) Construction of DR-PMSM

After reviewing various radial flux PMSMs and their ability to implement field weakening effectively, Bremner's machine design for DR-PMSM [4] was shortlisted. It has the capability to eliminate the back emf. Furthermore, those dual rotor arrangements can be implemented in both the applications with both surface magnet and interior magnet rotor structures.

The machine parameters investigated in this paper is shown below.

Parameter	Unit	Value
Machine Diameter	mm	800
Machine active length	mm	1000
Machine length	mm	1100
Rotor radius	mm	306
Airgap length	mm	10
Rotational Speed	rpm	115
Rated power	kW	410
Rated current	A	250
Poles	-	10
Stator slots	-	12
Winding layout	-	Double layer
Magnet length	mm	22
Remanent flux density	T	1.4

### FEM Modeling in COMSOL

To study all the subsequent phenomena occurring in DR-PMSM; such as eddy currents, non-linear characteristics of the machine, Torques, Forces and flux densities, FEA is the most accurate and feasible option compared to any analytical method. A 2D FEM model can be implemented for conventional PMSM and machine performance can easily be studied. During machine operation, hot spots in stator are due to eddy currents, which necessitated the need for 3D FEM.

A laminated structure of the iron core inside the PMSM requires modeling of an-isotropic material

which can only be modelled in 3D. To model the machine in 3D there were some simplifying assumptions made:

1. The material used in the machine model are linear.
2. The resistance is not included.
3. Laminations are modeled anisotropically in terms of permittivity and conductivity tensors
4. There are no eddy current losses considered in the rotor yoke and magnets.
5. The losses in the machine have not been considered.

### Geometry

The geometry was made using the built-in features of COMSOL Multiphysics 5.2 a. There was special care taken to model the stator conductors as double layer windings is used. The airgap was composed of three rings to study torques and axial forces. The gap between the two rotors was modeled as one of the rotor has the capability of shifting.

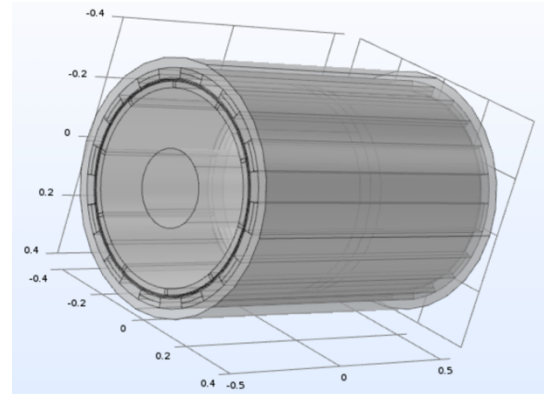


Figure 3 3D model geometry of DR-PMSM

### Material Properties

The geometry of the DR-PMSM demands that air should be in the gap between of the two rotors and this can be easily specified. The conductivity of air is redefined to 10 S/m, to receive a stable solution

Similarly, for magnets, rotor and stator iron and coils materials are specified from the built-in material properties from the library. Permeability and conductivity is the parameter describing the material included in COMSOL. The rotor yoke permeability is constant and rotor conductivity is assumed to be negligible to reduces computations time.

The permeability of the winding conductors and the airgap is given as scalar quantities. For the stator iron, it is not that straight forward. To model lamination, not every sheet can be included in 3D. So, a permeability

tensor and a conductivity tensor are defined for the stator iron. The stacking factor is 0.95 and the relative permeability for iron is 5000 and conductivity is  $1.12E+7$ . The tensors are used as follows:

$$\mu = \begin{bmatrix} 4750 & 0 & 0 \\ 0 & 4750 & 0 \\ 0 & 0 & 19.3 \end{bmatrix} \sigma = \begin{bmatrix} 1.064e7 & 0 & 0 \\ 0 & 1.064e7 & 0 \\ 0 & 0 & 19.9 \end{bmatrix}$$

### Defining Physics

The built-in feature *Rotating Machinery, Magnetic* physics node is used. The rotor back iron, magnets and the airgap domain is set up with magnetic scalar potential. The stator core and the coils domain is set up with magnetic vector potential. The equation used are:

$$\nabla \times \left( \frac{1}{\mu} \nabla \times \vec{A} \right) = \vec{J}$$

$$\nabla^2 \vec{A} = -\mu\sigma \left( -\nabla V - \frac{\partial \vec{A}}{\partial t} \right)$$

In the mixed formulation region, the regions of scalar potential are described by

$$-\nabla \cdot (\mu \nabla \phi) = 0$$

The magnetic insulation boundary is automatically set, assuming no flux to leave the machine.

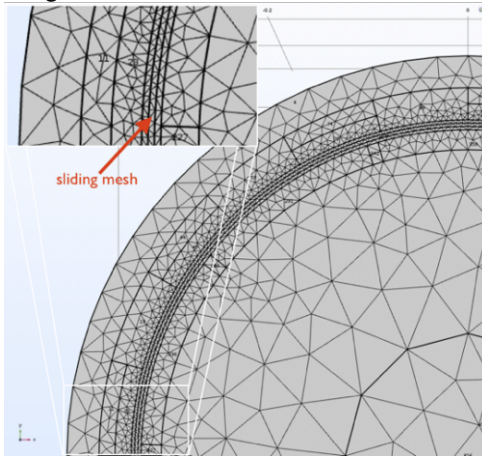


Figure 4 Meshing in the 3D machine model

As COMSOL uses Maxwell stress tensor for calculating forces, the correct integration surface is crucial. The surface for force calculation node should be inside the prescribed rotation velocity boundary surface. For accuracy, rings are added in the airgap while making the geometry, so that the element size can be controlled while meshing.

In this paper, the 3D model was large. However, an iterative solver could not be used since both vector and

scalar potentials gave a non-symmetric algebraic equation requiring a more robust direct solver.

### Simulation Results

The focuses for the simulation of the dual rotor PMSM are:

1. Validity of the machine
2. Induced voltages in the coils
3. Forces acting on the rotor
4. Flux in the stator iron.

#### 1. Validity of the machine model

In order to be sure that the modelled machine is generating the right results, it was compared to a conventional PMSM with the same parameters. If a DR-PMSM is in normal state, i.e. the magnets are not shifted, it should behave as a conventional PMSM. A 2D finite element model of conventional PMSM was therefore established in COMSOL. The induced voltages of both the machines are compared at no load and at loaded conditions. As seen from Figure 5 and 6, that the induced voltage is around 1100 V and the terminal voltage is around 1200 V for DR-PMSM. We observe similar voltage levels in Figure 7 and 8, which shows conventional PMSM's induced and terminal voltages. The ripple in the voltages of DR-PMSM simulations is because of a coarse mesh.

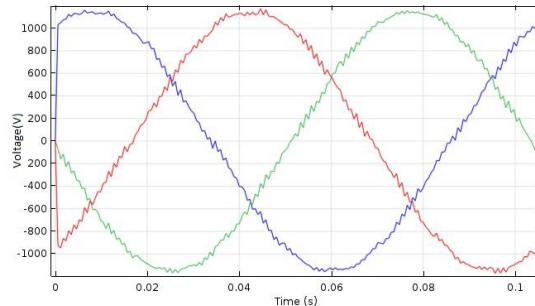


Figure 5 Induced Voltage at no load conditions

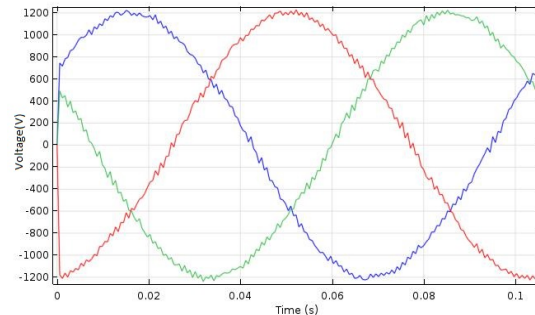


Figure 6 Terminal Voltage at no-load conditions

The next thing to be observed is the power in the machine. To confirm the machine model's validity, the power balance in the electrical machine should

hold, which means that mechanical power must be equal to electrical power.

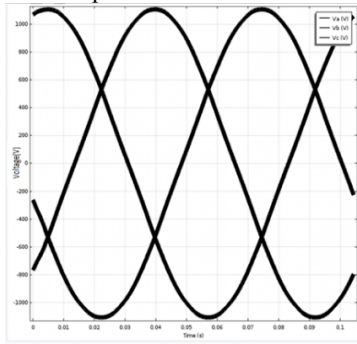


Figure 7 Induced voltage at no load conditions

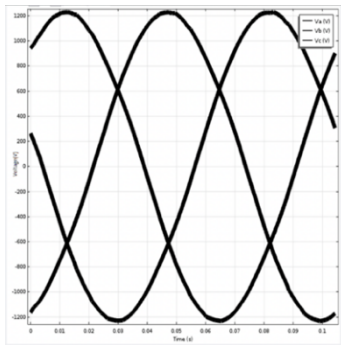


Figure 8 Terminal voltage at no load conditions

It can be mathematically written as:

$$T_e \omega = V_a I_a + V_b I_b + V_c I_c$$

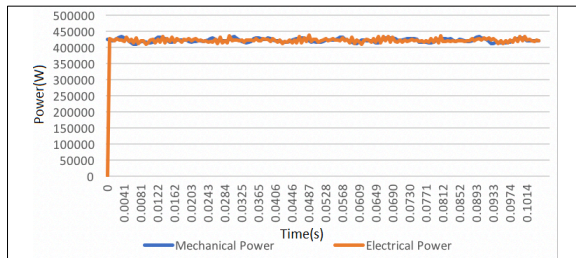


Figure 9 Mechanical and electrical power for DR-PMSM

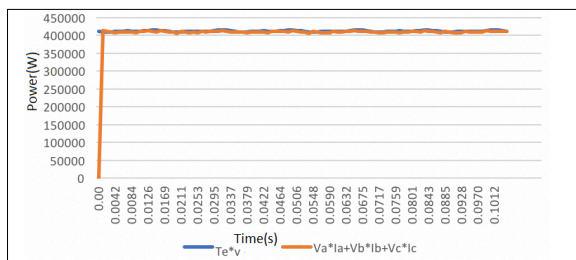


Figure 10 Mechanical and electrical power for conventional-PMSM

Figure 9 and 10 shows that mechanical power and electrical power of the DR- PMSM model, both are around 0.41 MW. This is also true for the conventional

PMSM model. Both the machine models hold the power balance which confirm their validity.

## 2. Effect of voltages in the coils

To confirm that the DR-PMSM reduces the induced voltages to zero by flux weakening, simulations were performed by shifting the magnets by 180 degrees electrically, with no load and loaded conditions. In Figure 12, when the machine is not loaded, the voltages have dropped drastically to a mere 1-2 V. The phasors diagram in Figure 13a, shows that the DR-PMSM at normal conditions behaves exactly like conventional PMSM.

When the machine is shifted by 180 degrees the voltage induced goes to zero as expected as shown in Figure 13b. The phasors show that the only voltage that remains in the machine is due to the currents in the stator windings which can be seen in Figure 12.

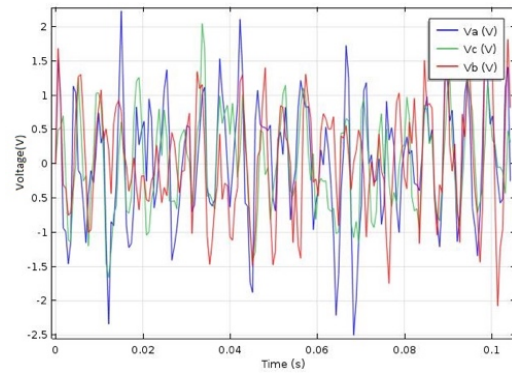


Figure 11 Induced voltage at loaded conditions for DR-PMSM

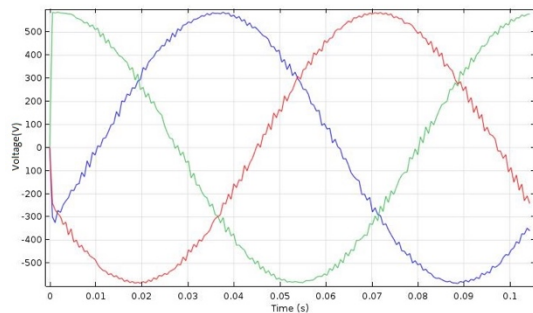


Figure 12 Terminal voltage at loaded conditions for DR-PMSM

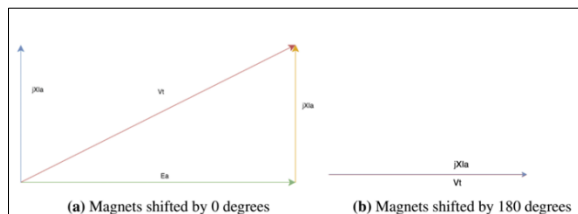


Figure 13 Phasor diagram: Terminal voltages, induced voltages for phase A of DR-PMSM



To observe the effect on voltage by field weakening in DR-PMSM, a simulation was carried out at different rotor positions and maximum voltages were computed. The voltages at 0 mechanical degrees is 1150 V and the voltage at 36 mechanical degrees is almost 0 V.

The reduction of voltages by flux weakening can be observed clearly in the plot between various rotor position and maximum voltages in Figure 14.

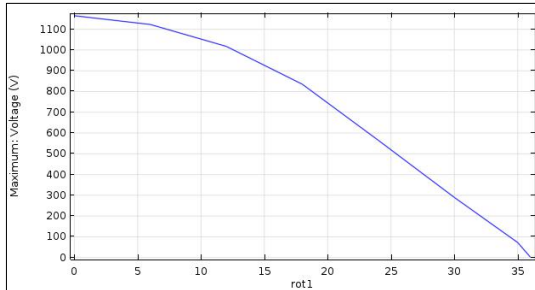


Figure 14 Voltages in phase A at various rotor positions

It can be concluded that DR-PMSM has the ability to completely reduce the flux to zero by field weakening.

### 3. Effect of forces

The Force calculation nodes were set up on both rotors, and axial forces were calculated using Maxwell stress tensor. To understand how these forces interact, the forces acting upon the two rotors are dealt in two cases; with no load case and with rated currents in the coils case.

#### Case 1: No load case

Figure 15 shows that the two rotors repel each other by the equivalent forces of 300 N and Figure 16 shows

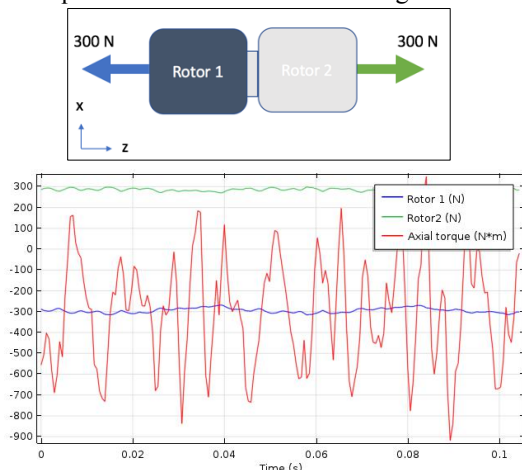


Figure 15 No load case: Axial forces on rotors and torque when the magnets are shifted by 0 degrees

that equivalent amount of attractive forces of 2500 N, are present when magnets are shifted by 180 degrees.

The red curve defines the high cogging torque in the machine, even when the rotors are misaligned, we observe the similar amount of cogging torque.

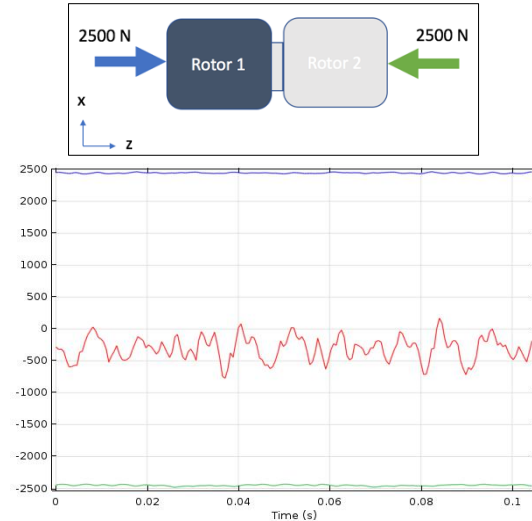


Figure 16 No load case: Axial forces on rotors and torque when the magnets are shifted by 180 degrees

#### Case 2: Loaded case

Similarly, in the case where there is current in the conductors, it can be seen in Figure 17 that the magnitude of forces has increased to 1800 N and the two rotors repel each other. The red curve indicates that torque in the machine which is around 35kNm. Furthermore, in the case of 180 degrees shifted magnets, it can be seen in Figure 18 that the two rotors attract each other with a higher magnitude of forces. These forces that repel each other are not equal because of the currents in the windings.

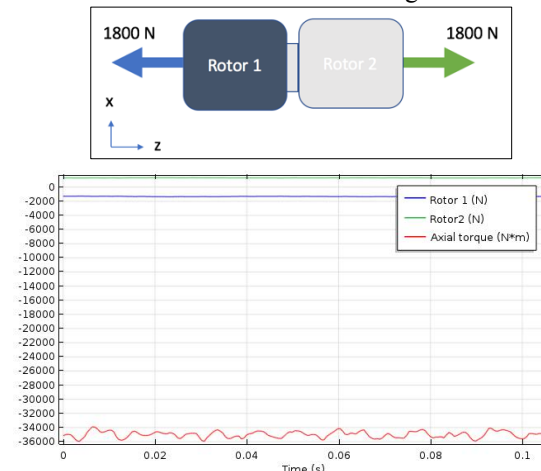


Figure 17 Loaded case: Axial forces on rotors and torque when the magnets are shifted by 0 degrees

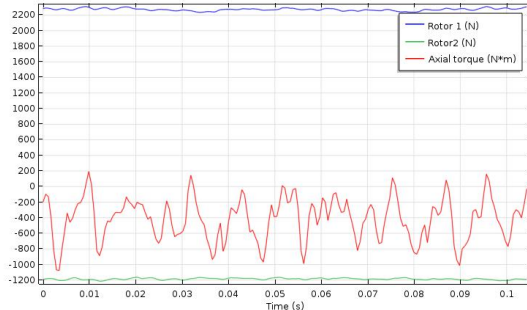
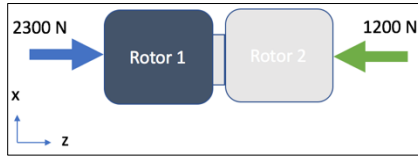


Figure 18 Loaded case: Axial forces on rotors and torque when the magnets are shifted by 180 degrees

It has been observed that there are attractive and repulsive forces between the two rotors, which makes it crucial to understand the forces on the rotors for the shifting mechanism. For this, a different set of simulations was carried out on a standstill rotor.

#### Axial Torques on the Rotor

In this simulation, axial torques were calculated on the individual rotors while one of the rotors were shifted from 0-360 degrees electrically at no load, stationary conditions while the other rotor is at standstill.

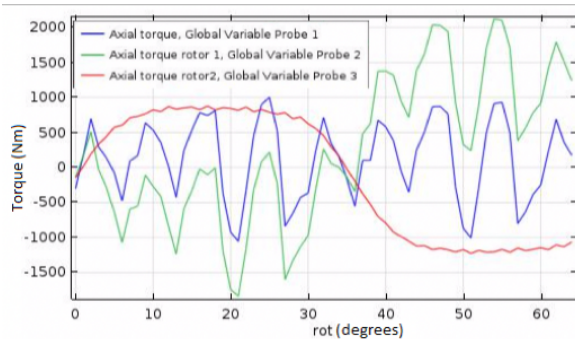


Figure 19 Axial torques on the rotors and the stator

In Figure 19, the blue curve shows the torque on the stator when one of the rotors is moved 360 degrees. As expected, we observe the cogging in the machine due to stator slot teeth and the poles. The red curve describes the forces experienced by the standstill rotor. As seen in the figure the red curve is not experiencing any cogging torque, the only forces affecting it are from the adjacent rotor due to the change in the magnetic fields by realignment of the magnets. While the green curve represents the forces on the moving rotor which clearly has both cogging and forces acting on it from the adjacent rotor. After analyzing the torques in Figure 19, it can be concluded that if

machine cogging is reduced the forces on the moving rotor can be reduced drastically.

#### 4. Flux in the stator

The DR-PMSM's construction enables it to control flux by realigning the magnets in the rotor. This makes the flux an important topic of discussion. In a normal situation, when magnets are not realigned, most of the flux passes through the stator radially. The lamination in the machine is modeled by the help of permeability and conductivity tensors. The machine radial airgap flux density  $B_r$  is observed in Figure 20. The dips on the peaks of the wave form are due to the stator teeth. The flux lines are more concentrated on the edge of stator teeth. The fundamental harmonic of the  $B_r$  wave can be seen even with the inclusion of the peaks and dips of the curve.

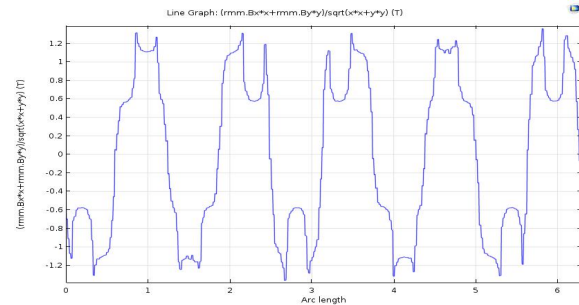


Figure 20 Airgap flux density on rotor 1 of DR-PMSM

The flux in the axial direction becomes a problem when the magnets are realigned by 180 degrees. The flux will tend to pass from north to south pole, and parts of the flux in the middle region of the stator (Figure 21) will pass orthogonally to the laminations. This will induce eddy currents in the stator iron. The following analysis is performed in the middle of the stator, because the flux in the axial direction is concentrated in that region.

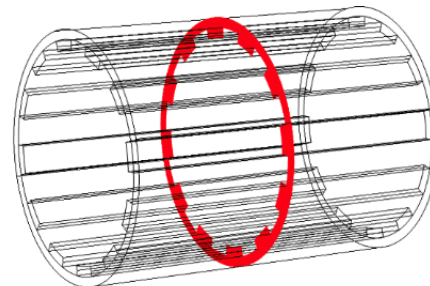


Figure 21 Middle part of the stator

Initially, when magnets are realigned by 180 degrees the flux is concentrated in the middle part of the stator as shown in Figure 22. Later, as the two rotors are allowed to rotate (for 57.4 milliseconds), the change in axial flux and eddy currents can be observed in Figure 23

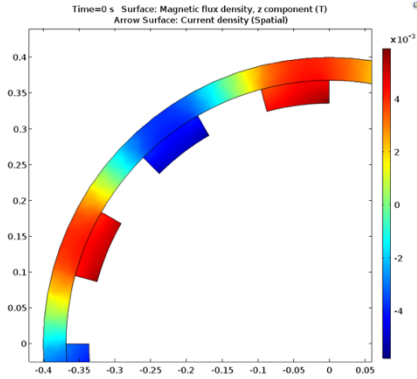


Figure 22  $B_z$  in the middle part of the stator at stationary, stand still conditions

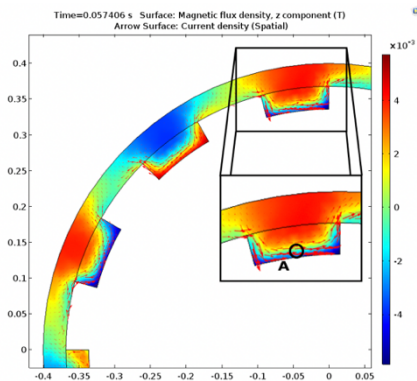


Figure 23  $B_z$  in the middle part of the stator at  $t = 57.4$  ms

The first thing to observe is where the magnetic flux density ( $B_z$ ) is concentrated and how it changes with time. Secondly, the induced eddy currents, depicted by arrows, oppose the change in  $B_z$ . The surface plot of ( $B_z$ ), in zoomed part of the Figure 23, shows that most  $B_z$  is concentrated in the tooth of the stator. This plot is taken at a time instant of 0.057406s and the observed  $B_z$  at point A is continuously changing which influences the eddy current flow in the stator

To observe the eddy current flow, a surface current density norm plot at time instant 0.52174s has been presented in Figure 24. This shows that currents are mostly concentrated around the edge of the stator teeth and the magnitude of the current is not as large in other parts. The direction and intensity of the currents is quite visible from the plot. The maximum magnitude of the current is around 40 A/mm<sup>2</sup>; just concentrated on the edges of the stator teeth.

The analysis shows that the middle part of the stator iron which is between the two rotors has some eddy current losses. To avoid these losses, a stator with a gap can be made for this machine. The windings are continuous but a spacer, having material of zero relative permeability, in the middle part of the stator

should be introduced in the design, making the windings a bit longer.

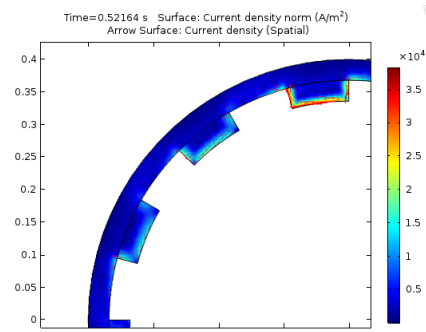


Figure 24 Change in directions of currents w.r.t current density norm

One cannot conclude on the severity of these losses from the simulations but the phenomenon of eddy current can be clearly observed in the realigned machine and needs more research.

## Conclusion

After the 3D FEA of DR-PMSM the following conclusions were drawn from simulation result.

- The efficiency of DR-PMSM is similar to a conventional PMSM.
- Induced voltages can be reduced to zero by the flux weakening mechanism in DR-PMSM.
- The forces on the rotors due to the shifting mechanism can be minimized by reducing cogging in the machine.
- Axial flux components in the machine induce certain hot spots in the middle part of the stator (between the gap of the two rotors), which should be further studied.

## References

- [1] Z. Daneshi-Far, G. A. Capolino, and H. Henao, "Review of failures and condition monitoring in wind turbine generators," in *The XIX International Conference on Electrical Machines - ICEM 2010*, 2010, pp. 1–6.
- [2] O. V. Thorsen and M. Dalva, "A survey of faults on induction motors in offshore oil industry, petrochemical industry, gas terminals, and oil refineries," *IEEE Trans. Ind. Appl.*, vol. 31, no. 5, pp. 1186–1196, Sep. 1995.
- [3] D. V. Spyropoulos and E. D. Mitronikas, "A Review on the Faults of Electric Machines Used in Electric Ships," *Advances in Power Electronics*, 2013.
- [4] R. D. Bremner, "Dual rotor electromagnetic machine," US7576465 B2, 18-Aug-2009.